

# Natural Variation of Root Hydraulics in *Arabidopsis* Grown in Normal and Salt-Stressed Conditions<sup>1[C][W]</sup>

Moira Sutka<sup>2,3</sup>, Guowei Li<sup>2</sup>, Julie Boudet<sup>4</sup>, Yann Boursiac, Patrick Doumas, and Christophe Maurel\*

Biochimie et Physiologie Moléculaire des Plantes, Institut de Biologie Intégrative des Plantes, UMR 5004 CNRS/UMR 0386 INRA/Montpellier SupAgro/Université Montpellier 2, F-34060 Montpellier cedex 2, France (M.S., G.L., J.B., Y.B., P.D., C.M.); and Diversité et Adaptation des Plantes Cultivées, Equipe Rhizogénèse, UMR 188 Institut de Recherche pour le Développement/INRA/Montpellier SupAgro/Université Montpellier 2, F-34394 Montpellier cedex 5, France (P.D.)

To gain insights into the natural variation of root hydraulics and its molecular components, genotypic differences related to root water transport and plasma membrane intrinsic protein (PIP) aquaporin expression were investigated in 13 natural accessions of *Arabidopsis* (*Arabidopsis thaliana*). The hydraulic conductivity of excised root systems ( $L_{pr}$ ) showed a 2-fold variation among accessions. The contribution of aquaporins to water uptake was characterized using as inhibitors mercury, propionic acid, and azide. The aquaporin-dependent and -independent paths of water transport made variable contributions to the total hydraulic conductivity in the different accessions. The distinct suberization patterns observed among accessions were not correlated with their root hydraulic properties. Real-time reverse transcription-polymerase chain reaction revealed, by contrast, a positive overall correlation between  $L_{pr}$  and certain highly expressed *PIP* transcripts. Root hydraulic responses to salt stress were characterized in a subset of five accessions (Bulhary-1, Catania-1, Columbia-0, Dijon-M, and Monte-Tosso-0 [Mr-0]).  $L_{pr}$  was down-regulated in all accessions except Mr-0. In Mr-0 and Catania-1, cortical cell hydraulic conductivity was unresponsive to salt, whereas it was down-regulated in the three other accessions. By contrast, the five accessions showed qualitatively similar aquaporin transcriptional profiles in response to salt. The overall work provides clues on how hydraulic regulation allows plant adaptation to salt stress. It also shows that a wide range of root hydraulic profiles, as previously reported in various species, can be observed in a single model species. This work paves the way for a quantitative genetics analysis of root hydraulics.

An efficient uptake of soil water by roots is crucial to meet the water demand for shoot transpiration and growth. Because of its coupling to ion uptake, root water transport is also central to mineral nutrition of the whole plant. The water transport capacity of the root, that is, its hydraulic conductance ( $L_0$ ), therefore, is a key physiological parameter. It is determined by both the root architecture and its intrinsic water per-

meability (hydraulic conductivity [ $L_{pr}$ ]). Studies in numerous plant species have shown that  $L_0$  is under tight environmental and physiological control. For instance, the availability of water, nutrients, or oxygen in the soil can induce short-term (minutes to hours) changes in  $L_{pr}$  and longer term (hours to days) changes in root architecture (Steudle, 2000; Vandeleur et al., 2005; del Martínez-Ballesta et al., 2006; Maurel et al., 2010).

Hydraulic regulation is fundamental to plant water relations because it determines the interplay between water flow intensity and water potential gradients throughout the plant body. This regulation can affect integrated responses such as stomatal movements or growth control under changing environmental conditions (Christmann et al., 2007; Parent et al., 2009; Ache et al., 2010). Hydraulic regulation can directly be addressed using molecular and physiological approaches with individual cells or organs. The role of water channel proteins (aquaporins) and their regulation as related to hydraulic conductivity have been the subject of intense research (Vandeleur et al., 2005; Maurel et al., 2008). Plasma membrane intrinsic proteins (PIPs), which are divided into two subgroups (PIP1 and PIP2) with five and eight isoforms, respectively, represent the most abundant aquaporins in the root plasma membrane in *Arabidopsis* (*Arabidopsis thaliana*). The plasma membrane plays a central role in

<sup>1</sup> This work was supported by the Agence Nationale de la Recherche (grant no. ANR-05-GPLA-034-06) and by the Agropolis Fondation (Montpellier, France) through a fellowship to G.L.

<sup>2</sup> These authors contributed equally to the article.

<sup>3</sup> Present address: Laboratorio 2, Departamento de Biodiversidad y Biología Experimental, Facultad de Ciencias Exactas y Naturales, Universidad de Buenos Aires, Intendente Güiraldes 2160 Piso 4 (C1428EGA), Buenos Aires, Argentina.

<sup>4</sup> Present address: Génétique, Diversité et Ecophysiologie des Céréales, UMR 1095 INRA/Université Blaise Pascal, Campus des Cézeaux, 24 avenue des Landais, BP 80026, F-63171 Aubière, France.

\* Corresponding author; e-mail maurel@supagro.inra.fr.

The author responsible for distribution of materials integral to the findings presented in this article in accordance with the policy described in the Instructions for Authors ([www.plantphysiol.org](http://www.plantphysiol.org)) is: Christophe Maurel ([maurel@supagro.inra.fr](mailto:maurel@supagro.inra.fr)).

[C] Some figures in this article are displayed in color online but in black and white in the print edition.

[W] The online version of this article contains Web-only data.

[www.plantphysiol.org/cgi/doi/10.1104/pp.110.163113](http://www.plantphysiol.org/cgi/doi/10.1104/pp.110.163113)

controlling transcellular water transport (Steudle and Peterson, 1998). The contribution of the whole PIP1 and PIP2 subfamilies and of individual PIP1 and PIP2 isoforms to root water uptake has been established by reverse genetics approaches in tobacco (*Nicotiana tabacum*) and *Arabidopsis* (Martre et al., 2002; Siefritz et al., 2002; Javot et al., 2003; Postaire et al., 2010). In addition, transcriptional and posttranslational regulation, including stimulus-induced trafficking or gating of PIP aquaporins, have recently been described in roots under water, anoxic, and oxidative stress conditions (Vandeleur et al., 2005; del Martínez-Ballesta et al., 2006; Maurel et al., 2008). Water transport across living tissues can also involve the apoplast (Steudle and Peterson, 1998), although the molecular bases and genetic control of this path are somewhat less understood. Yet, it was recently shown that suberin deposition in specialized root cell layers (exodermis and endodermis), which may affect root water transport properties, can vary between genotypes (Baxter et al., 2009) and physiological contexts (Melchior and Steudle, 1993; Zimmermann et al., 2000; Vandeleur et al., 2009). In addition, fully differentiated xylem vessels usually provide, with respect to radial hydraulic conductance, a nonlimiting axial conductance. Yet, protoxylem vessels can be limiting for water uptake near the root tip (Steudle and Peterson, 1998; Bramley et al., 2009).

Large-scale natural genetic variation and quantitative trait locus mapping have been reported for integrated water relation parameters (Nienhuis et al., 1994; McKay et al., 2003; Poormohammad Kiani et al., 2007; Bouchabke et al., 2008; Collins et al., 2008) but, to our knowledge, not for plant tissue hydraulic properties. Information on the hydraulic properties of different tissues or organs might nevertheless be very important for plant breeding. In addition, gene discovery enabled by quantitative genetics approaches may prove in the long term more powerful than reverse genetics in identifying new molecular determinants of plant hydraulics. In fact, root water transport has so far been compared in a restricted number (three or fewer) of rice (*Oryza sativa*), maize (*Zea mays*), or grapevine (*Vitis vinifera*) varieties (Aroca et al., 2001; Miyamoto et al., 2001; Yu et al., 2006; Matsuo et al., 2009; Vandeleur et al., 2009). Aquaporin gene expression was also recently investigated in five *Arabidopsis* accessions, but independently of plant hydraulic properties (Alexandersson et al., 2010). Thus, the aim of this article was to evaluate further the potential of intraspecific natural variation for studying the hydraulic strategies of plants under normal and water stress conditions. We tried to go beyond classical, pair-wise comparisons between genetically distinct lines to perform more powerful correlation analyses. Considering that *Arabidopsis* represents a model angiosperm for exploring intraspecific natural variation, we investigated genotypic differences related to root water transport in a series of 13 natural accessions of this species. To support our extensive physiological characterizations, we also investigated several molecular and cellular

aspects that possibly underlie the hydraulic properties of plant roots. The overall work provides clues on how hydraulic regulation allows plant adaptation to a changing environment. It also paves the way for a quantitative genetics analysis of root hydraulics.

## RESULTS

### Selection and Growth of Accessions

Accessions were selected without any a priori consideration of their natural habitat, including geographical distribution or precipitation levels. Rather, we maximized the genetic variation in a restricted number of isolates and chose the nested core collection of eight accessions defined by McKhann et al. (2004): Bulhary-1 (Blh-1), Burren-0 (Bur-0), Catania-1 (Ct-1), Cape Verde Islands-0 (Cvi-0), Ibel Tazekka-0 (Ita-0), St Jean Cap Ferrat (Jea), Oystese-0 (Oy-0), and Shahdara (Sha). The Antwerpen-1 (An-1), Dijon-M (Di-M), and Monte-Tosso-0 (Mr-0) accessions were also selected because of their contrasting response to water stress (Granier et al., 2006; M. Sutka and C. Maurel, unpublished observations). The Columbia-0 (Col-0) and Landsberg *erecta* (*Ler*) accessions, which are commonly used for generating recombinant inbred line populations, were also included as references in our study. Previous work has shown that the selected accessions vary in their life cycle and growth properties and, in particular, in the time of floral induction and final number of rosette leaves (McKhann et al., 2004; Granier et al., 2006; Bouchabke et al., 2008). To minimize these differences, studies were performed on 17- to 27-d-old plants; that is, at an early stage of their growth phase. Hydroponic cultures were used as a source of intact root systems, a prerequisite for characterization of root hydraulics. When grown at standard temperature and under long days (16 h), all plants achieved consistent growth rates, with mean individual dry weights (mg  $\pm$  SE) of roots ( $DW_r$ ) and shoots ( $DW_s$ ) varying between  $3.7 \pm 0.3$  (An-1) and  $6.4 \pm 0.9$  (Cvi-0 and Sha) and between  $16.2 \pm 0.9$  (Ita-0) and  $40.4 \pm 5.9$  (Sha), respectively (Table I). At the end of the culture, most accessions were in vegetative growth, but floral buds were observed in some others. At this stage, none of the accessions showed signs of senescence.

### Natural Variation of Root Hydraulic Conductivity

Pressure-induced sap flow [ $J_v(P)$ ; Tournaire-Roux et al., 2003] was used to characterize water transport in whole roots excised from plants of all accessions. The deduced linear pressure-to-flow relationships are indicative of  $L_0$  (Table II).  $L_0$  reflects the overall water uptake capacity of the root and is contributed by both the root exchange surface and its intrinsic water transport capacity ( $L_{p,r}$ ). To accurately determine the latter parameter, mean root diameter and length were measured and integrated to whole root surface (Table I). Mean  $L_{p,r}$  values (Fig. 1) showed significant variation

**Table I.** Morphological parameters of *Arabidopsis* plants

*Arabidopsis* plants of the indicated accessions were germinated and grown in vitro for 10 d and further grown in hydroponic conditions for 11 d as described in "Materials and Methods." The mean  $DW_s$  and  $DW_r$  values were measured, and their ratio ( $DW_s/DW_r$ ) was calculated from the ratio of individual plants. The morphology of roots was characterized through measurements of root diameters ( $d_r$ ; mean or median values), overall root length ( $L_r$ ), and surface area ( $S_r$ ). The mean  $S_r/DW_r$  ratio was determined by linear regression from a  $S_r$ -to- $DW_r$  plot. The number of individual root segments ( $d_r$ ) or plants (all parameters) used is indicated in parentheses. Plants from at least two independent cultures were used. Values shown are means  $\pm$  SE.

Accession	$DW_s$	$DW_r$	$DW_s/DW_r$	$d_r$ (Mean)	$d_r$ (Median)	$L_r$	$S_r$	$S_r/DW_r$
	mg			$\mu\text{m}$		m	$10^{-3} \text{ m}^2$	$\text{m}^2 \text{ g}^{-1}$
An-1	24.4 $\pm$ 1.7 (16)	3.7 $\pm$ 0.3 (16)	6.9 $\pm$ 0.4 (16)	130.9 $\pm$ 1.5 (464) (4)	128.8 (464) (4)	4.6 $\pm$ 0.4(4)	1.9 $\pm$ 0.2 (4)	0.62 (4)
Blh-1	27.1 $\pm$ 2.7 (28)	5.1 $\pm$ 0.5 (28)	5.4 $\pm$ 0.2 (28)	123.7 $\pm$ 1.5 (503) (5)	122.6 (503) (5)	6.8 $\pm$ 1.2 (5)	2.7 $\pm$ 0.5 (5)	0.61 (5)
Bur-0	37.3 $\pm$ 3.7 (17)	6.1 $\pm$ 0.6 (17)	6.2 $\pm$ 0.3 (17)	132.5 $\pm$ 1.8 (369) (4)	128.3 (369) (4)	5.0 $\pm$ 1.3 (4)	2.1 $\pm$ 0.5 (4)	0.50 (4)
Col-0	27.0 $\pm$ 3.8 (19)	5.0 $\pm$ 0.6 (19)	5.3 $\pm$ 0.3 (19)	123.3 $\pm$ 1.4 (469) (5)	117.0 (469) (5)	6.8 $\pm$ 2.0 (5)	2.7 $\pm$ 0.8 (5)	0.66 (5)
Ct-1	34.2 $\pm$ 3.8 (18)	4.8 $\pm$ 0.4 (18)	7.1 $\pm$ 0.4 (18)	129.9 $\pm$ 1.6 (490) (5)	125.6 (490) (5)	5.0 $\pm$ 1.7 (5)	2.0 $\pm$ 0.7 (5)	0.57 (5)
Cvi-0	29.9 $\pm$ 2.8 (15)	6.4 $\pm$ 0.6 (15)	5.0 $\pm$ 0.3 (15)	131.0 $\pm$ 1.6 (363) (4)	130.1 (363) (4)	5.5 $\pm$ 1.4 (4)	2.3 $\pm$ 0.5 (4)	0.57 (4)
Di-M	30.6 $\pm$ 2.8 (36)	4.9 $\pm$ 0.4 (36)	6.3 $\pm$ 0.2 (36)	133.8 $\pm$ 1.6 (468) (5)	127.6 (468) (5)	5.9 $\pm$ 2.2 (5)	2.5 $\pm$ 0.9 (5)	0.64 (5)
Ita-0	16.2 $\pm$ 0.9 (23)	4.2 $\pm$ 0.2 (23)	3.9 $\pm$ 0.1 (23)	138.8 $\pm$ 1.3 (634) (6)	136.6 (634) (6)	5.6 $\pm$ 0.4 (6)	2.4 $\pm$ 0.2 (6)	0.54 (6)
Jea	29.8 $\pm$ 3.1 (16)	5.6 $\pm$ 0.5 (16)	5.3 $\pm$ 0.2 (16)	126.3 $\pm$ 1.4 (462) (4)	121.1 (462) (4)	3.8 $\pm$ 1.1 (4)	1.3 $\pm$ 0.4 (4)	0.53 (4)
Ler	30.3 $\pm$ 3.3 (15)	5.4 $\pm$ 0.7 (15)	5.9 $\pm$ 0.2 (15)	128.3 $\pm$ 1.6 (469) (5)	128.0 (469) (5)	4.5 $\pm$ 0.8 (5)	1.9 $\pm$ 0.2 (5)	0.68 (5)
Mr-0	20.0 $\pm$ 1.5 (24)	4.1 $\pm$ 0.3 (24)	5.0 $\pm$ 0.2 (24)	143.0 $\pm$ 1.8 (493) (5)	135.3 (493) (5)	7.3 $\pm$ 2.6 (5)	3.5 $\pm$ 1.4 (5)	0.53 (5)
Oy-0	34.1 $\pm$ 3.7 (14)	5.6 $\pm$ 0.6 (14)	6.3 $\pm$ 0.5 (14)	132.9 $\pm$ 2.0 (368) (4)	126.6 (368) (4)	6.7 $\pm$ 1.8 (4)	2.8 $\pm$ 0.6 (4)	0.63 (4)
Sha	40.4 $\pm$ 5.9 (14)	6.4 $\pm$ 0.9 (14)	6.2 $\pm$ 0.3 (14)	131.6 $\pm$ 1.6 (369) (4)	128.6 (369) (4)	6.1 $\pm$ 1.3 (4)	2.6 $\pm$ 0.5 (4)	0.65 (4)

between accessions, with an approximately 2-fold difference ( $P = 0.003$  and  $P = 0.012$ ) between extremes (Blh-1,  $Lp_r = 3.69 \pm 0.39 10^{-8} \text{ m s}^{-1} \text{ MPa}^{-1}$ , on the one hand; Di-M,  $Lp_r = 7.27 \pm 1.11 10^{-8} \text{ m s}^{-1} \text{ MPa}^{-1}$ , and Ct-1,  $Lp_r = 7.20 \pm 0.71 10^{-8} \text{ m s}^{-1} \text{ MPa}^{-1}$ , on the other hand).

Assuming that root length instead of root surface could be limiting during water uptake, we also calculated  $Lp_r$  based on root length. The classification profile of the 13 accessions was barely changed, with again a 2-fold difference ( $P = 0.003$  and  $P = 0.023$ ) between the same extremes (Blh-1,  $Lp_r = 1.49 \pm 0.22 10^{-11} \text{ m}^2 \text{ s}^{-1} \text{ MPa}^{-1}$ , on the one hand; Di-M,  $Lp_r = 3.00 \pm 0.75 10^{-11} \text{ m}^2 \text{ s}^{-1} \text{ MPa}^{-1}$ , and Ct-1,  $Lp_r = 2.89 \pm 0.40 10^{-11} \text{ m}^2 \text{ s}^{-1} \text{ MPa}^{-1}$ , on the other hand).

### Contribution of Aquaporins to Water Uptake

The contribution of aquaporins to  $Lp_r$  was explored by means of inhibitors, which although not fully specific exhibit distinct modes of action. Mercury, a general aquaporin blocker, acts by oxidation and binding to accessible Cys residues, thereby blocking and/or collapsing the aqueous pore (Daniels et al., 1996; Hirano et al., 2010). Propionic acid and azide both induce an intracellular acidosis, by acid loading or blocking of respiration via the cytochrome pathway respiration, respectively (Tournaire-Roux et al., 2003). This, in turn, leads to  $\text{H}^+$ -dependent gating of PIPs (Tournaire-Roux et al., 2003; Törnroth-Horsefield et al., 2006; Verdoucq et al., 2008). Time courses of exposure of roots to 50  $\mu\text{M}$   $\text{HgCl}_2$ , 20 mM propionic acid, pH 6.0, or 1 mM  $\text{NaN}_3$  were characterized in individual plants. In all cases, and as described for Col-0 (Tournaire-Roux et al., 2003; Postaire et al., 2007), maximal inhibition of  $J_v(P)$  was achieved in less than 40 min. Figure

2 shows, for the 13 accessions, the mean percentage of  $Lp_r$  inhibition after the three treatments. Mercury reduced  $Lp_r$  by 34%  $\pm$  5% (Bur-0) to 64%  $\pm$  3% (An-1). Propionic acid had a comparable effect and blocked  $Lp_r$  by 30%  $\pm$  3% (Blh-1) to 67%  $\pm$  4% (Ita-0). Although different relative inhibition of  $Lp_r$  by the two molecules could be observed for certain accessions, their effects were significantly ( $P < 0.05$ ) correlated among accessions ( $r = 0.56$ ), supporting the idea that the two molecules targeted a common mechanism. By comparison with those two inhibitors, azide was even more effective and blocked  $Lp_r$  by up to 77%  $\pm$  2% (Ita-0). Also, propionic acid and azide showed very

**Table II.** Root water transport capacity of plants grown in standard conditions

Root hydraulic conductance ( $L_0$ ) was derived from either  $J_v$  measurements at 0.32 MPa ( $n = 7-19$ ) or linear  $J_v(P)$  relationships ( $n = 4-14$ ; see "Materials and Methods"). Mean values  $\pm$  SE from the indicated number of plants ( $n$ ), from at least three independent cultures, are shown.

Accession	$L_0$	$n$
	$\mu\text{L s}^{-1} \text{ MPa}^{-1}$	
An-1	0.118 $\pm$ 0.010	27
Blh-1	0.155 $\pm$ 0.018	33
Bur-0	0.159 $\pm$ 0.015	29
Col-0	0.196 $\pm$ 0.021	27
Ct-1	0.199 $\pm$ 0.021	29
Cvi-0	0.151 $\pm$ 0.015	27
Di-M	0.208 $\pm$ 0.017	34
Ita-0	0.103 $\pm$ 0.009	16
Jea	0.126 $\pm$ 0.011	27
Ler	0.187 $\pm$ 0.015	25
Mr-0	0.111 $\pm$ 0.013	23
Oy-0	0.240 $\pm$ 0.018	24
Sha	0.237 $\pm$ 0.023	25

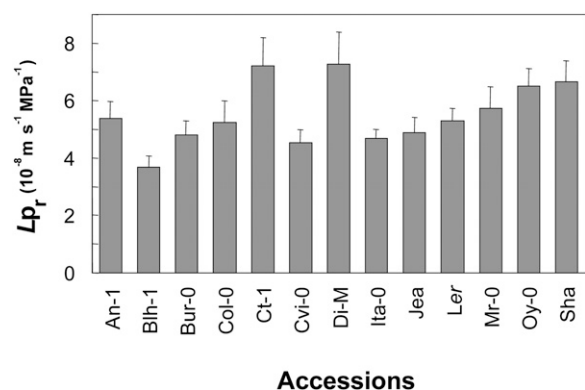


**Figure 1.**  $L_{p_r}$  of Arabidopsis accessions grown in standard conditions.  $L_{p_r}$  of individual plants was derived from the ratio of root hydraulic conductance ( $L_0$ ) to root surface ( $S_r$ ). Mean values  $\pm$  SE of the number of plants indicated in Table I are shown. A one-way ANOVA indicated significant differences between the  $L_{p_r}$  of Blh-1 and those of Ct-1 ( $P = 0.012$ ) and Di-M ( $P = 0.003$ ).

similar inhibition profiles among the 13 accessions (Fig. 2;  $r = 0.76$ ), in agreement with their common mode of action. Overall, the three inhibitory treatments provide converging evidence to estimate the relative contribution of aquaporins to  $L_{p_r}$ .

We noted, however, that among the 13 accessions, there was no significant correlation between  $L_{p_r}$  and its relative inhibition by any one of the three treatments (Supplemental Fig. S1). This suggests that pathways other than aquaporins can make a significant contribution to  $L_{p_r}$ . To evaluate the absolute contribution of the inhibitable versus residual  $L_{p_r}$  components, we examined, in each individual accession, the absolute effects of the three  $L_{p_r}$ -inhibiting treatments (Supplemental Fig. S2). Considering the  $L_{p_r}$  values that were blocked by mercury, propionic acid, or azide, Bur-0 and Blh-1 had the two lowest sensitivities, whereas inhibition values for Ct-1, Di-M, Mr-0, and Sha were among the five highest with any one of the inhibitors. This criterion allows us to distinguish two subgroups of accessions with a low (Bur-0 and Blh-1) or a high (Ct-1, Di-M, Mr-0, and Sha) contribution of aquaporins to  $L_{p_r}$ . Considering the residual  $L_{p_r}$  value after treatment by mercury, propionic acid, or azide, Bur-0, Ct-1, Di-M, and Oy-0 were in all cases among the five highest. By contrast, other accessions, such as An-1, Ita-0, Mr-0, and to a lesser extent Blh-1, showed very low residual  $L_{p_r}$  values after exposure to each of these inhibitors. This suggests that the aquaporin-independent paths in the first (Bur-0, Ct-1, Di-M, and Oy-0) and second (An-1, Blh-1, Ita-0, and Mr-0) subgroups are larger (more conductive) and smaller (tight), respectively. Overall, our analysis points to marked differences between accessions in both the aquaporin-dependent and -independent paths. As these differences can be independently observed among accessions, the work reveals a large natural variation in hydraulic profiles in the Arabidopsis root.

## Principal Component Analysis of Plant Hydraulics

To have a more global view of the hydraulic strategies developed by various accessions, we performed a principal component analysis (PCA) of the morphological (Table I),  $L_0$  (Table II),  $L_{p_r}$  (Fig. 1), and aquaporin inhibition (Fig. 2) data gathered in the 13 selected accessions. Figure 3A shows the correlation circle generated by the first two principal components. The first principal component (PC1), which can account for approximately 44% of the total variation in the data set, is contributed positively by plant growth characteristics ( $DW_s$ ,  $DW_r$ ) and negatively by aquaporin-dependent hydraulic conductivity, the relative inhibition by the three aquaporin inhibitors showing a clear clustering. The second principal component (PC2; approximately 29% of total variation) is contributed by overall root hydraulic parameters,  $L_{p_r}$  and  $L_0$ , and the shoot-to-root ratio ( $DW_s/DW_r$ ). Such clustering is consistent, as a high  $DW_s/DW_r$  induces a high demand on root hydraulics.

Projection of the 13 accessions on the first factorial (PC1/PC2) plane (Fig. 3B) resulted in a large scattering, confirming the variety of their hydraulic strategies. Yet, this and the analyses above allow identifying accessions with marked differences. Blh-1, which has the lowest  $L_{p_r}$  and a tight aquaporin-independent path, clusters with Bur-0, which also exhibits a relatively low  $L_{p_r}$  associated with a more conductive

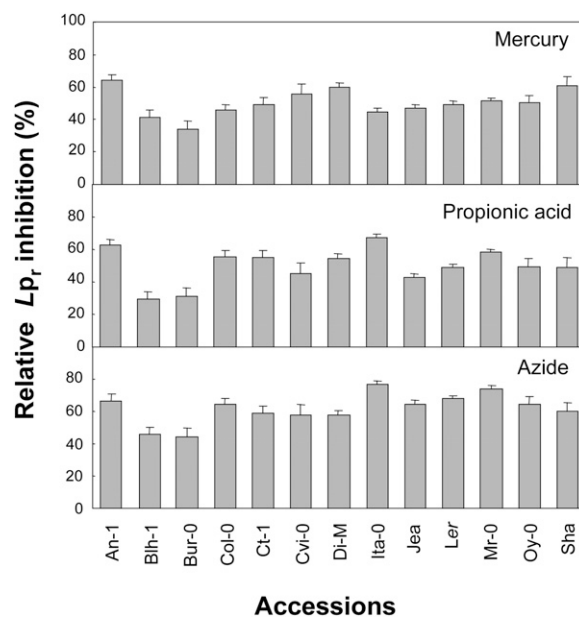


**Figure 2.** Relative inhibition of  $L_{p_r}$  by aquaporin-inhibiting treatments. Roots excised from plants grown in standard conditions were inserted in a pressure chamber, and  $J_v(P)$  was measured before and after treatment with  $50 \mu\text{M}$   $\text{HgCl}_2$  (Mercury),  $20 \text{ mM}$  propionic acid, pH 6.0 (Propionic acid), or  $1 \text{ mM}$   $\text{NaN}_3$  (Azide). For each treatment, the mean relative inhibition  $\pm$  SE of  $L_{p_r}$  was deduced from kinetic measurements on five to seven plants from at least two independent cultures.

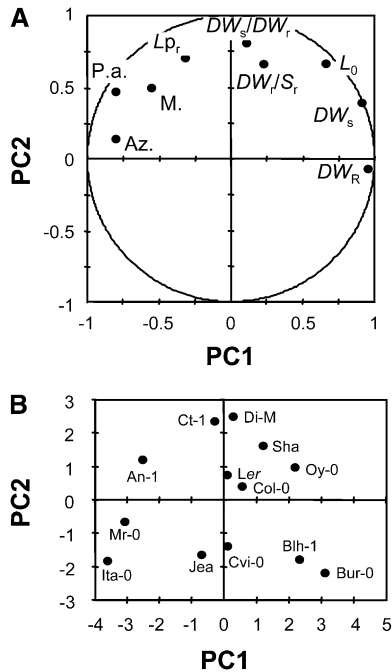


**Figure 3.** PCA of root hydraulics and of root and shoot growth in 13 *Arabidopsis* accessions. A, Plot of the first PCA plane on a correlation circle. The first (PC1) and second (PC2) axes contribute to 43.7% and 28.8% of the total variation, respectively. The measured parameters are named according to Table I and Table II except for the percentage of  $Lp_r$  inhibition by mercury, propionic acid, and azide, which are referred to as M., P.a., and Az., respectively. B, Repartition of accessions on the first PCA plane.

aquaporin-independent path. By contrast, Mr-0 and An-1 have a higher  $Lp_r$  but a tighter aquaporin-independent path. Ct-1 and Di-M show an even higher  $Lp_r$  due to a high conductance of both of the aquaporin-dependent and -independent paths.

#### Aquaporin Expression Profiles

To explore further the natural variation of aquaporin function in the *Arabidopsis* root, we investigated the abundance of aquaporin transcripts using quantitative real-time reverse transcription (Q-RT)-PCR. Expression of the 13 individual *PIP* genes was probed in the 13 selected accessions and was normalized to expression of the same gene in Col-0. The resulting gene profiles are shown in Figure 4 and Supplemental Figure S3. The plant genotype had a significant effect ( $P < 0.01$ ) on transcript abundance of all *PIP* genes except *PIP1;3* and *PIP2;1*. Overall, we found a few (five) genes including *PIP1;3* with a low relative variation of transcript abundance ( $\sigma_{RE}$ ; less than 0.3). Two of these (*PIP1;2*,  $\sigma_{RE} = 0.20$ ; *PIP2;2*,  $\sigma_{RE} = 0.20$ ) are among the most highly expressed isoforms in Col-0 roots (Alexandersson et al., 2005; Boursiac et al., 2005). By contrast, the expression profile of *PIP2;1* was remarkable, as its transcript abundance in Col-0 was 4- to 19-fold higher than in any of the 12 other accessions

(Fig. 4). Also, expression of *PIP1;4*, *PIP2;6*, *PIP2;7*, and *PIP2;8* was very low in some accessions (Fig. 4; Supplemental Fig. S3).

To explore the idea that variation in  $Lp_r$  among accessions could be the result of allelic variation in *PIP* expression levels, we investigated possible covariation between  $Lp_r$  and *PIP* transcript abundance. PCA revealed a rough positive correlation between  $Lp_r$  and certain highly expressed *PIP* genes, such as *PIP1;2* and *PIP2;2* (Fig. 5A). We failed, however, to reveal any significant positive correlation between  $Lp_r$  and the abundance of single *PIP* transcripts (Supplemental Table S1). The PCA also pointed to a marked negative correlation between  $Lp_r$  and the transcript abundance of *PIP2;6* and *PIP2;8* (Fig. 5A; Supplemental Table S1). Indeed, a negative linear correlation between *PIP2;8* transcript abundance and  $Lp_r$  could be resolved ( $r = -0.59$ ;  $P = 0.034$ ). A similar tendency was observed for *PIP2;6* ( $r = -0.43$ ;  $P = 0.14$ ), the best correlation being obtained between the mean abundance of *PIP2;6* and *PIP2;8* transcripts and  $Lp_r$  ( $r = -0.60$ ;  $P = 0.030$ ; Fig. 5B).

#### Root Anatomy

Root anatomy was also explored as a major determinant of the water transport properties of the whole organ and of the aquaporin-independent path in particular. To investigate this in detail, we worked on a subset of accessions identified via the PCA (Fig. 3) and selected because of their contrasting root hydraulic properties. Ct-1 and Di-M, on the one hand, and Blh-1, on the other hand, represent accessions with the highest and lowest  $Lp_r$  values, respectively. We also selected Mr-0 as an accession with intermediate  $Lp_r$  values but an apparently tight aquaporin-independent path. Col-0, which has been extensively characterized, both anatomically and physiologically, was taken as a reference accession.

The radial cellular organization and presence of apoplastic barriers were investigated in cross-sections of mature roots taken at 3 to 20 mm from the tip. All root sections exhibited at least two xylem vessels with a diameter greater than 7  $\mu\text{m}$ , and no significant difference in vascular tissue morphology was observed between accessions. Suberin deposition (Casparian strips) was observed after Sudan IV staining in the endodermis cell walls of all five accessions (Fig. 6A). These deposits were the most prominent in Blh-1 and least prominent in Ct-1 and Mr-0. By contrast, roots of the latter two accessions showed pronounced neutral lipid deposition in the outermost cell walls of their roots. Suberized periderms have been described in *Arabidopsis* roots with a secondary structure (Höfer et al., 2008) and provide an additional barrier for water and/or ion movements. We noted that the distinct suberization patterns among accessions are not correlated with their root hydraulic profiles and, in particular, with the tightness of the aquaporin-independent path.

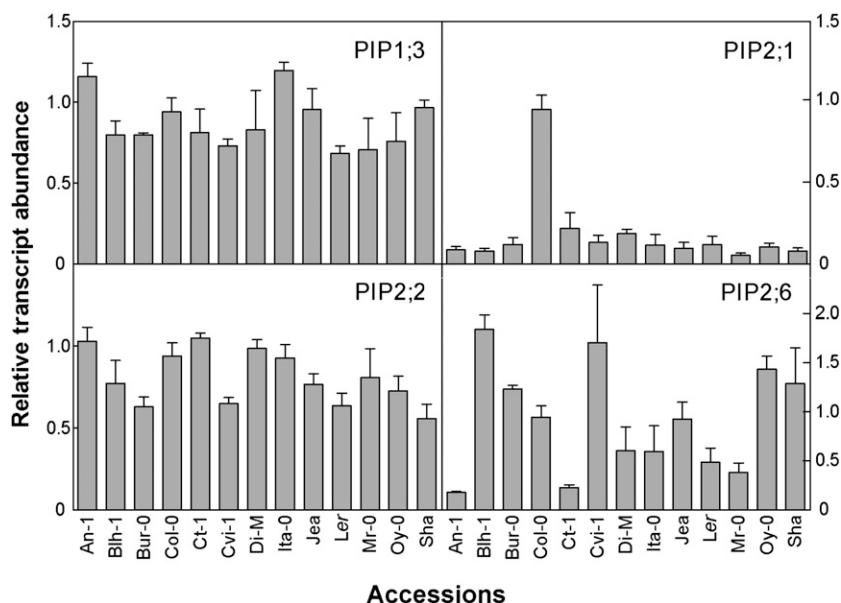


**Figure 4.** Relative transcript abundance of four representative *PIP* genes in 13 accessions. Transcript abundance of the indicated *PIP* genes was measured by Q-RT-PCR as described in “Materials and Methods” and was normalized to expression of the same gene in Col-0. The figure shows four representative *PIP* genes with either low  $\sigma_{RE}$  (*PIP1;3*,  $\sigma_{RE} = 0.19$ ; *PIP2;2*,  $\sigma_{RE} = 0.20$ ) or with a very high (*PIP2;1*) or very low (*PIP2;6*;  $\sigma_{RE} = 0.61$ ) expression in a few accessions. Data from two independent biological experiments (plant cultures), each with duplicate PCRs, are shown. Note that PCR efficiency was checked for each *PIP* gene amplification and in each accession. Although the *PIP* primers were designed in Col-0, the high abundance of the *PIP2;1* transcripts in this accession cannot be explained by a sequence mismatch between Col-0 and the other accessions.

Within each accession, and in relation to the root diameter, we also observed a significant variation in the number of endodermal and cortical cell files, which varied between eight and 12 and between seven and 12, respectively (Fig. 6). In addition, and at variance with the canonical root structure described in most root developmental studies, the addition of a second cortical cell layer, previously described as middle cortex (Baum et al., 2002; Paquette and Benfey, 2005), was observed in some root sections. Because additional cortical cells derive from periclinal division of individual endodermal cells, the new layer may not be complete. Overall, the formation of a middle cortex could be observed in all accessions but was the most pronounced in Ct-1 and Mr-0 and the least pronounced in Col-0. Therefore, it was not linked to any specific root hydraulic profile.

#### Response of Organ and Cell Hydraulic Conductivity to Salt Stress

Differences in root anatomy and/or hydraulic profiles suggested that it could be interesting to investigate the responses of *Arabidopsis* accessions to water and/or ionic stress. Salinity, which combines these two types of stresses, exerts marked effects on *Arabidopsis* root water transport. For instance, exposure for 3 to 4 h of Col-0 roots to 100 mM NaCl reduces their  $L_{pr}$  by  $63\% \pm 3\%$  (Boursiac et al., 2005). The effects of the same treatment were investigated in the four other accessions of the selected subset. In all cases,  $L_{pr}$  was deduced from accurate  $J_v(P)$  relationships, the consistency of salt effects being checked from a shift of the balancing pressure  $P_0$  to more positive values (Boursiac et al., 2005). Consistent with the response observed in Col-0, the  $L_{pr}$  of Blh-1, Ct-1, and Di-M was reduced by a 100 mM NaCl treatment, but with distinct ampli-

tudes, to (in percentage of control value)  $63\% \pm 17\%$  ( $n = 10$ ) in Ct-1 and  $30\% \pm 13\%$  ( $n = 7$ ) in Di-M (Fig. 7). In strong contrast, the  $L_{pr}$  of Mr-0 did not show any significant variation in response to salt ( $169\% \pm 25\%$ ;  $n = 11$ ; Fig. 7).

Cell responses to salinity were investigated by pressure probe measurements in the root cortex. Although cortical cells are amenable to this technique under control or aquaporin-inhibiting conditions (Javot et al., 2003; Tournaire-Roux et al., 2003; Boursiac et al., 2008), our investigation proved very challenging, as the 100 mM NaCl treatment induced a calculated drop in stationary turgor ( $P_e$ ) of approximately 0.5 MPa, thereby precluding any stable cell measurement. We found, however, that after 4 h of salt exposure, cortical cells were punctually able to restore  $P_e$  to values of approximately 0.2 MPa. Primary cell water relation parameters ( $P_e$ , half-time of hydrostatic relaxation, and volumetric elastic modulus) could then be acquired, under standard or salt stress conditions, in the root cortex of the five selected accessions (Supplemental Table S2). The deduced cell hydraulic conductivity ( $L_{p_{cell}}$ ) values are shown in Figure 8. In standard conditions, and irrespective of their mean  $L_{pr}$  values, the five accessions exhibited similar  $L_{p_{cell}}$  in the range of 1 to  $1.4 \cdot 10^{-6} \text{ m s}^{-1} \text{ MPa}^{-1}$ . Consistent with the salt-induced down-regulation of  $L_{pr}$ , Blh-1, Col-0, and Di-M showed a significant reduction in  $L_{p_{cell}}$  to (in percentage of control values)  $70\% \pm 9\%$  ( $n = 21$ ;  $P = 0.04$ ),  $79\% \pm 8\%$  ( $n = 20$ ;  $P = 0.04$ ), and  $73\% \pm 7\%$  ( $n = 21$ ;  $P = 0.01$ ), respectively. By contrast, Ct-1 and Mr-0 showed no significant variation of  $L_{p_{cell}}$  in response to salt (Ct-1,  $136\% \pm 17\%$  [ $n = 14$ ]; Mr-0,  $116\% \pm 16\%$  [ $n = 17$ ]). The lack of  $L_{p_{cell}}$  inhibition in these two accessions may be related to the moderate inhibition and lack of salt-induced inhibition of  $L_{pr}$  in Ct-1 and Mr-0, respectively. The overall data show contrasting strat-

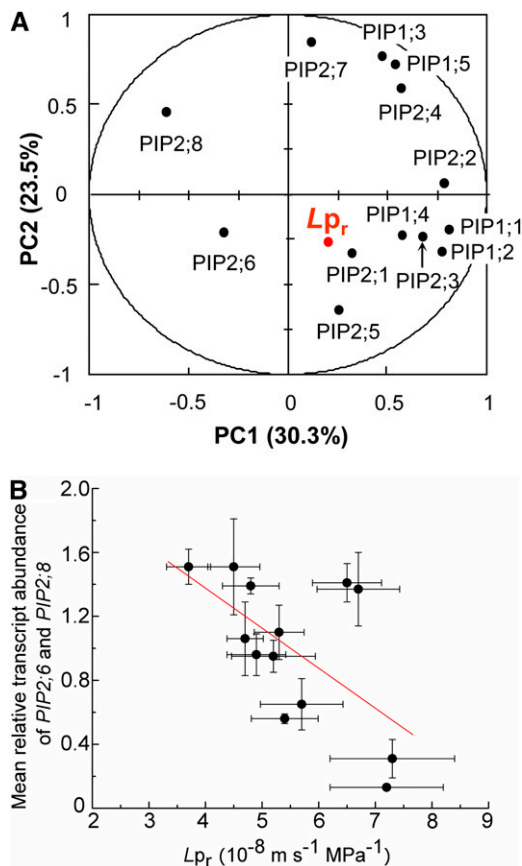


**Figure 5.** Genetic covariation of  $Lp_r$  and *PIP* transcript abundance. A, PCA of  $Lp_r$  and *PIP* transcript abundance in roots of 13 *Arabidopsis* accessions. The figure shows the plot of the first PCA plane on a correlation circle. The relative contributions (in percentage) to the total variation of the first (PC1) and second (PC2) axes are indicated in parentheses. The data used are those shown in Figure 1 ( $Lp_r$ ) and Figure 4 and Supplemental Figure S3 (*PIP* transcript abundance). B, Negative linear correlation between  $Lp_r$  and the transcript abundance of *PIP2:6* and *PIP2:8*. The figure shows a plot of mean  $Lp_r$  against the mean summed transcript abundance (TA) of *PIP2:6* and *PIP2:8* in each of 13 accessions. The linear regression line is  $TA = a \times Lp_r + b$ , with  $a = 2.40 \pm 0.57$  and  $b = -0.25 \pm 0.1$ . The derived Pearson correlation factor is  $R_{\text{Pearson}} = -0.60$ , with  $sd = 0.38$  and  $P = 0.030$ . [See online article for color version of this figure.]

egies among accessions for root water transport regulation in response to salt stress, both at the cell and whole organ levels.

### Aquaporin Regulation under Salt Stress

Previous studies in Col-0 have shown that the mid- to long-term (greater than 2 h) inhibition of  $Lp_r$  by salt is accompanied by a reduced abundance of the most highly expressed *PIP* and *TIP* transcripts (Martínez-Ballesta et al., 2003; Boursiac et al., 2005). To compare such transcriptional regulation to the varying  $Lp_r$  responses in the five selected accessions, we measured in parallel the transcript abundance of all 13 *PIP* genes

and of four abundantly expressed *TIP* genes (*TIP1:1*, *TIP1:2*, *TIP2:2*, *TIP2:3*). Transcripts for the *TIP* and the most highly expressed *PIP* (*PIP1:1*, *PIP1:2*, *PIP2:1*, *PIP2:2*) genes showed, for the five investigated accessions, reduced or punctually stable abundance after a 4-h treatment of roots by 100 mM NaCl (Fig. 9). A slight salt-induced accumulation of other transcripts (*PIP1:4*, *PIP2:5*, *PIP2:6*) was also observed in most accessions, consistent with previous transcriptional analyses of drought-stressed plants (Alexandersson et al., 2005, 2010). Although Blh-1 showed a tendency to lower inhibition and higher stimulation, the five accessions showed qualitatively similar transcriptional profiles in response to salt (Fig. 9). More specifically, all transcripts showed similar salt-induced variation profiles within the five accessions, except the *PIP1:1* and *PIP2:2* transcripts, the abundance of which was significantly more reduced in Mr-0 than in Blh-1 (*PIP1:1*,  $P = 0.01$ ; *PIP2:2*,  $P = 0.046$ ).

## DISCUSSION

### A Diversity of Hydraulic Profiles in the *Arabidopsis* Root

Although considerable variation in root hydraulics has been long identified among plant species (Steudle and Peterson, 1998; Rieger and Litvin, 1999; Bramley et al., 2009), the genetic bases of this trait have only been addressed by reverse genetics (Martre et al., 2002; Siefritz et al., 2002; Javot et al., 2003; Postaire et al., 2010) or by comparison of a restricted number (two or three) of plant cultivars (Aroca et al., 2001; Miyamoto et al., 2001; Yu et al., 2006; Matsuo et al., 2009; Vandeleur et al., 2009). Here, we have applied state-of-the-art molecular and biophysical techniques to a broader set of *Arabidopsis* accessions to gain further insights into the natural variation of root hydraulics and of its molecular components. By describing a substantial (2-fold) genetic variation of  $Lp_r$ , we first established that root hydraulic properties are far from uniform in this species. The calculation of  $Lp_r$  from  $L_{or}$ , however, relies on assumptions regarding the factor limiting water uptake. In this work,  $Lp_r$  was referenced to the whole root surface, assuming that outer cell layers consistently reflected the hydraulic properties of all segments of the root system. We also checked that when  $Lp_r$  was referenced to root length or root tip numbers (data not shown), a similar 2-fold difference among accessions was observed, with Blh-1 and Di-M always exhibiting the two extreme values.

To get a further insight into these  $Lp_r$  variations, the contribution of aquaporins was explored using converging effects of three inhibitors with distinct modes of action. Our data indicate that the absolute contribution of both the aquaporin-dependent and -independent paths showed significant and independent variation. Thus, a large variety of hydraulic profiles could be observed that parallels those previously uncovered between species (Steudle and Peterson,

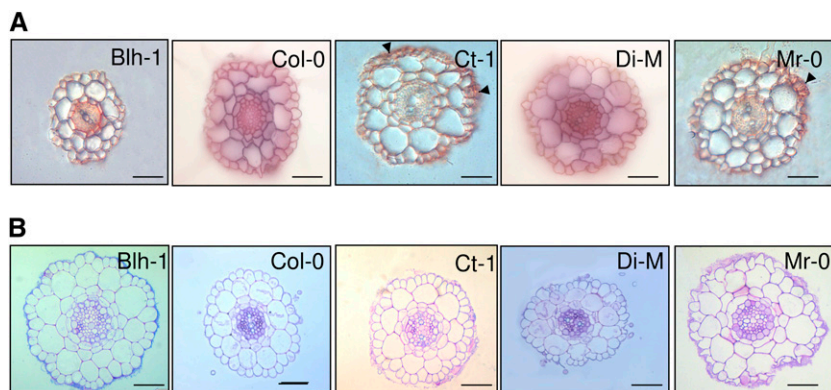


**Figure 6.** Transverse root anatomy of five selected accessions. A, Sudan IV-stained cross-sections taken at 3 to 8 mm behind the root tip. Red-stained suberin can be observed in the cell walls of endodermal cells. Arrowheads show marked lipid deposition in the outermost cell walls of Ct-1 and Mr-0. B, Toluidine blue-stained cross-sections taken at 15 to 20 mm behind the root tip. The sections show the presence of a partial or full second layer of cortical cells. Note that Blh-1 can show root segments with a single-layer (A) or a full double-layer (B) root cortex. None of the other accessions shows a full double-layer cortex. Bars = 50  $\mu\text{m}$ .

1998; Rieger and Litvin, 1999; Bramley et al., 2009). As examples, Blh-1 exhibited the lowest  $L_{p_r}$  while Bur-0 had a slightly higher  $L_{p_r}$  due to a more conductive aquaporin-independent path. Col-0 and Mr-0 exhibited intermediate  $L_{p_r}$  values, with a tighter aquaporin-independent path in the latter accession. Ct-1 and Di-M showed an even higher  $L_{p_r}$  due to a high conductance of both of the aquaporin-dependent and -independent paths (Figures 1 and 2; Supplemental Fig. S2).

#### Molecular and Cellular Bases of Root Water Transport

The natural variation of root hydraulics may first be accounted for by variations in tissue organization and/or cell wall structure. For instance, suberization of apoplastic barriers has classically been associated with root maturation and reduced water uptake capacity (Melchior and Steudle, 1993; Zimmermann and Steudle, 1998). Although Arabidopsis accessions showed significant variation in their root anatomy, we did not observe any clear link between root suberization and the hydraulic conductivity of the aquaporin-independent path. Similarly, a lack of correlation between endodermis and exodermis suberization and  $L_{p_r}$  was already pointed out by Rieger and Litvin (1999) when comparing five species with marked differences in root anatomy. Our study also did not reveal any marked difference in vascular tissue morphology between Arabidopsis accessions. This does not exclude, however, that xylem vessels marginally contribute to the root hydraulic resistance, in the apical parts in particular. Overall, a comprehensive understanding of Arabidopsis root hydraulic architecture integrating anatomical and morphological parameters, as was attempted in species with larger roots (Bramley et al., 2009), is still needed.

Aquaporins represent an obvious potential molecular determinant of root hydraulics. Numerous studies have explored the variations of  $L_{p_r}$  and aquaporin expression within a unique plant genotype but under changing physiological conditions (Henzler et al., 1999; Boursiac et al., 2005; Mahdieh et al., 2008). The observed covariations have emphasized the role of aquaporin transcription in the long-term control of

root hydraulics under stress conditions. This conclusion has been confirmed by a few recent studies where aquaporin expression was compared in a pair of rice and a pair of grapevine cultivars (Yu et al., 2006; Vandeleur et al., 2009). Here, we have explored the genetic variation of *PIP* gene expression and its relationship to  $L_{p_r}$  in a larger set of accessions. We specifically wondered whether allelic variations in transcript abundance of a single *PIP* may be robust determinants of  $L_{p_r}$  or, more generally, whether distinct expression profiles might identify haplotypic groups linked to specific root hydraulic architectures.

In line with previous work by Alexandersson et al. (2010) and with public gene expression (Affymetrix data (<http://www.bar.utoronto.ca/efp/cgi-bin/efpWeb.cgi>), our work indicates a significant natural variation in *PIP* transcript abundance. Although  $L_{p_r}$  or its relative sensitivity to aquaporin blockers was in gen-

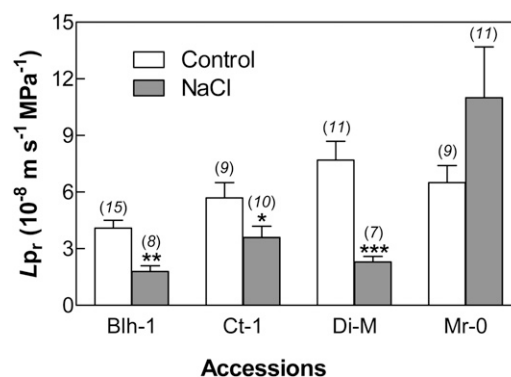


**Figure 7.** Effects of a salt treatment on  $L_{p_r}$ . Plants from the indicated accessions were either maintained in standard hydroponic conditions or exposed for 4 h to a standard hydroponic nutrient solution supplemented with 100 mM NaCl, and  $L_{p_r}$  was measured, in the absence (Control) or in the presence of salt (NaCl), as described in "Materials and Methods." Mean values  $\pm$  SE from the indicated number of plants (in parentheses) and at least three independent plant cultures are shown. Asterisks indicate  $L_{p_r}$  in salt-treated plants that are significantly different from values in control conditions (\*  $P < 0.05$ , \*\*  $P < 0.01$ , \*\*\*  $P < 0.001$ ).



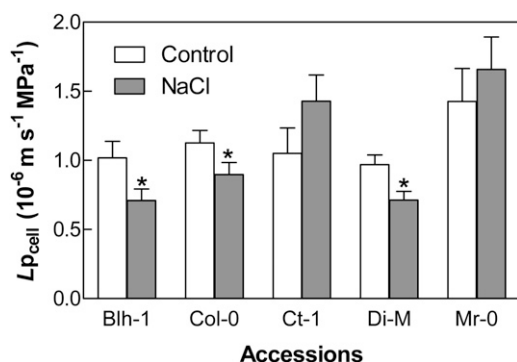


**Figure 8.** Effects of a salt treatment on  $L_{p_{cell}}$ . Plants from the indicated accessions were either grown in standard conditions or exposed for 4 h to a standard nutrient solution supplemented with 100 mM NaCl, as described in the legend to Figure 7. The excised root segment to be punctured was transferred into a cell pressure probe solution, either standard or complemented with 100 mM NaCl, for 10 to 40 min prior to measurement of  $L_{p_{cell}}$  in the root cortex. Mean values  $\pm$  SE from 16 cells (Control) and 14 cells (NaCl) and two to four independent plant cultures are shown. Asterisks indicate  $L_{p_{cell}}$  in salt-treated roots that are significantly different ( $P < 0.05$ ) from values in control conditions.

eral correlated with the overall *PIP* transcript abundance (Fig. 5A), no positive correlation with a specific isoform could be resolved (Supplemental Table S1). Thus, the statement that many quantitative trait loci can be explained by differences in gene transcription level rather than by changes in protein sequence or function (Collins et al., 2008) may not so simply apply to aquaporins, as these proteins are subjected to multiple posttranslational regulations (Chaumont et al., 2005; Maurel et al., 2008). Alternatively, more precise analyses in less varied genetic backgrounds may be required to uncover a positive link between  $L_{p_r}$  and the expression level of specific aquaporin genes. For instance, a tentative association between the plant water status (relative water content) and the expression of tonoplast aquaporins has been observed in two parental lines and four derived recombinant inbred

lines of sunflower (*Helianthus annuus*; Poormohammad Kiani et al., 2007).

Surprisingly, our data revealed a negative correlation between the transcript abundance of *PIP2;6* and *PIP2;8*, on the one hand, and  $L_{p_r}$  or its inhibitable component, on the other hand. This correlation is weak and will have to be confirmed on a larger set of data. It may be the result of fortuitous genetic linkage between the two types of characters or the effects of dominating pleiotropic factors acting on both of these. Yet, such a negative correlation may also reflect a true physiological covariation. A *PIP2;6* promoter-*GUS* transgene showed the expression of *PIP2;6* to be weak in roots and much stronger in flowers and in the vascular tissues of petioles and leaves (Alexandersson et al., 2010). This pattern suggests that cross-talk and a compensation between the hydraulics of roots ( $L_{p_r}$ ) and shoots (*PIP2;6* mRNA abundance) may contribute to optimal delivery of water into leaf tissues. By contrast to most other *PIP* genes that are down-regulated under water stress, *PIP2;6* shows a drought-insensitive and salt-induced transcription (Alexandersson et al., 2005, 2010; Fig. 9). Here again, enhanced expression of *PIP2;6* in roots and shoots may provide a mechanism for compensating for reduced soil water uptake under water-limiting conditions. Expression of *PIP2;8* is low in roots and leaves, somewhat higher in flowers (Jang et al., 2004; Alexandersson et al., 2005; Boursiac et al., 2005), dependent on light or abiotic stresses (Jang et al., 2004; Postaire et al., 2010), and was already shown to be highly variable among five accessions (Alexandersson et al., 2010). The lack of cell-specific expression data for *PIP2;8*, however, precludes further speculation on its function.

### Diversity of Salt Stress Responses

To explore further the genotypic variation of the Arabidopsis accessions, we characterized them under salt stress conditions and identified quantitative and, most importantly, qualitative differences in their salt-

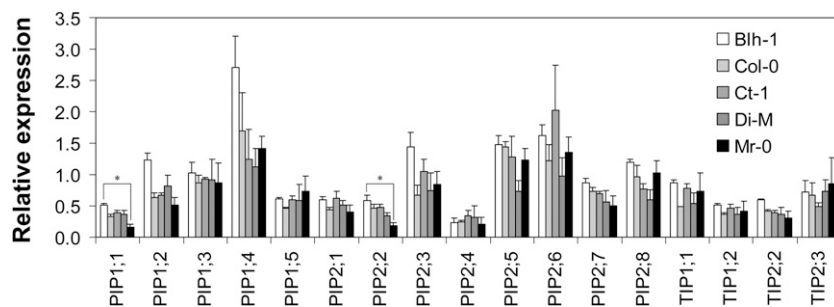


**Figure 9.** Effects of a salt treatment on aquaporin gene expression. The transcript abundance of the indicated genes was measured in roots from plants grown in standard conditions or exposed for 4 h to a 100 mM NaCl treatment. For the five accessions of interest, the aquaporin transcript abundance in salt-treated roots was plotted as the (fold) expression relative to standard conditions. Mean values  $\pm$  SE from three independent experiments (plant cultures), each with duplicate PCRs, are shown. Transcript abundances showed similar salt-induced variations within the five accessions, except for *PIP1;1* and *PIP2;2*, where they were more reduced in Mr-0 than in Blh-1 (*PIP1;1*,  $P = 0.01$ ; *PIP2;2*,  $P = 0.046$  [asterisks]).

induced regulations. Thus,  $Lp_r$  was down-regulated in all investigated accessions (Blh-1, Col-0, Ct-1, Di-M) except Mr-0. In this and the Ct-1 accession,  $Lp_{cell}$  was unresponsive to salt, whereas it was down-regulated in the three other accessions (Blh-1, Col-0, Di-M). Coordinated down-regulation of whole root and cell hydraulic conductivities is usually observed or expected in roots under stress (Steudle and Peterson, 1998; Steudle, 2000; Tournaire-Roux et al., 2003), but our results indicated that  $Lp_r$  and  $Lp_{cell}$  can vary independently. This observation is reminiscent of a study in grapevine, which showed that a drought-induced decrease in  $Lp_r$  was accompanied by an increase in cortex  $Lp_{cell}$  in a Chardonnay but not in a Grenache cultivar (Vandeleur et al., 2009). In addition, certain species such as barley (*Hordeum vulgare*) and tobacco do not adjust their  $Lp_r$  in response to salt stress (Munns and Passioura, 1984; Tyerman et al., 1989). This behavior and that of Mr-0 possibility reflect an anisohydric strategy for sustained growth under moderate water stress (Vandeleur et al., 2009). Thus, our work indicates that the variation of root hydraulic responses to water stress conditions, which was previously observed in pair-wise intraspecific comparisons (Aroca et al., 2001; Yu et al., 2006; Vandeleur et al., 2009) or between species, can be observed intraspecifically in a single model species. The ecological significance of the observed variation is not clear, however, as the root hydraulic profiles of the accessions selected for this study cannot simply be linked to their geographical dispersion. In addition, we have poor knowledge of the actual salinity and water availability in the habitats of these accessions.

### Molecular Physiology of Root Responses to Salt Stress

The distinct salt stress response profiles uncovered in the various accessions, however, point to differences in adaptive strategy. It is generally found that, under salt stress, a high root selectivity, that is, an efficient uptake of water without a passive salt influx, can be achieved through apoplastic suberin depositions, which specifically block ion diffusion (Steudle, 2000). This strategy may operate in Blh-1, Col-0, and Di-M, which had the most pronounced suberin deposition in the endodermis. In addition, a salt-induced reduction in  $Lp_r$  (and therefore reduced water uptake) is thought to prevent a passive drag of salt within root tissues (Maurel et al., 2010). With respect to the composite model of root water transport (Steudle and Peterson, 1998), it was somewhat surprising that the  $Lp_{cell}$  response of the cortex to salt was always of lesser amplitude than that of  $Lp_r$ . To explain this apparent paradox, we propose that cell-to-cell water transport is maintained or even favored in the outer cell layers to create a specific path for water uptake. Interestingly, this response was most pronounced in Ct-1 and Mr-0, which had lesser endodermis suberization. Other anatomical specializations may also be involved in differential root responses to salt stress and will require

closer inspection. For instance, middle cortex formation is repressed by *SCARECROW* and gibberellin (Paquette and Benfey, 2005). Its regulation along the root, that is, during root maturation, or in response to endogenous or environmental factors may vary between accessions to differentially adjust root hydraulics under normal or stress conditions.

Because of its lack of hydraulic response to salt, Mr-0 appears to be an interesting reference accession to investigate the mechanisms of stress-induced  $Lp_r$  regulation. Whereas the genetic variation of stress responses is often associated with the differential expression of stress-responsive genes (Chen et al., 2005; Collins et al., 2008), our analyses did not reveal any major difference in salt-induced regulation of aquaporin gene expression between this and the other accessions. A global conservation of drought-induced PIP regulation patterns has also been reported by Alexandersson et al. (2010) in another set of five *Arabidopsis* accessions. Thus, some basic pathways for response to water stress seem to be conserved within the whole species. Yet, the five accessions characterized in this work showed very distinct functional profiles, confirming, as indicated above, the predominance of posttranscriptional mechanisms for aquaporin regulation under normal or stress conditions (Boursiac et al., 2005, 2008). We thus anticipate that Mr-0 may lack some changes in salt-induced aquaporin phosphorylation and trafficking.

### CONCLUSION

Comparative physiology of various plant species under standard or stress conditions indicates that many factors contribute to root hydraulics (Steudle and Peterson, 1998; Rieger and Litvin, 1999; Bramley et al., 2009). Here, we show that each of these factors displays quantitative variation among *Arabidopsis* natural accessions, which, therefore, are a rich source of genetic variation for dissecting root hydraulics.

As a model species, *Arabidopsis* has been instrumental for developing novel quantitative genetics approaches and cloning the corresponding quantitative trait genes (QTGs; Alonso-Blanco et al., 2009; Atwell et al., 2010). While several QTGs involved in mineral nutrition or other important agronomic traits have recently been characterized (Alonso-Blanco et al., 2009), the molecular mechanisms that underlie the variety of water relation responses is emerging (Ren et al., 2010). By describing a significant genetic variation of root hydraulics, this work fulfills a prerequisite for future quantitative genetics analyses of this trait. The next challenge will be to develop high-throughput phenotyping methods to characterize mapping populations and see whether the natural variation in root hydraulics is genetically tractable. In addition, it remains unclear whether aquaporin genes can represent large-effect QTGs. Master regulators of a large number of genes may represent more relevant targets of quan-

titative genetics approaches. It is expected that signaling intermediates acting upstream of aquaporins and exerting powerful effects on overall tissue water relations can be identified by this approach.

## MATERIALS AND METHODS

### Plant Material and Culture Conditions

Seeds of natural accessions of *Arabidopsis* (*Arabidopsis thaliana*) were provided by the Department of Genetics and Plant Improvement, INRA, in Versailles, France (<http://dbsgap.verailles.inra.fr/vnat/>), except *Ler* seeds, which were supplied by the Nottingham Arabidopsis Stock Centre. In this study, we used the Nested Core Collection of eight accessions (Blh-1, Bur-0, Ct-1, Cvi-0, Ita-0, Jea, Oy-0, Sha [McKhann et al., 2004]; Versailles identification numbers 180AV, 172AV, 162AV, 166AV, 157AV, 25AV, 224AV, 236AV, respectively), two reference ecotypes (Col-0 [186AV] and *Ler* [NW20]), and three other accessions known for their typical response to water stress (An-1 [96AV], Mr-0 [148AV], and Di-M; Granier et al., 2006; M. Sutka and C. Maurel, unpublished observations). Seeds were surface sterilized and sown in clear polystyrene culture boxes (12 × 12 cm) on a standard culture medium [5 mM KNO<sub>3</sub>, 2 mM MgSO<sub>4</sub>, 1 mM Ca(NO<sub>3</sub>)<sub>2</sub>, 50 mM FeEDTA, microelements according to Murashige and Skoog (1962), 2.5 mM K<sub>2</sub>HPO<sub>4</sub> + KH<sub>2</sub>PO<sub>4</sub>, 1 mM MES, 10 g L<sup>-1</sup> Suc, and 7 g L<sup>-1</sup> agar, pH 6.1, adjusted with KOH]. The boxes were kept for 2 d at 4°C, incubated vertically for 10 d at 20°C in the light, and seedlings were transplanted into hydroponic culture. Plants were mounted on a 35 × 35 × 0.6-cm polystyrene raft floating on a basin filled with 8 L of hydroponic culture medium [1.25 mM KNO<sub>3</sub>, 0.75 mM MgSO<sub>4</sub>, 1.5 mM Ca(NO<sub>3</sub>)<sub>2</sub>, 0.5 mM KH<sub>2</sub>PO<sub>4</sub>, 50 mM FeEDTA, 50 mM H<sub>3</sub>BO<sub>3</sub>, 12 mM MnSO<sub>4</sub>, 0.70 mM CuSO<sub>4</sub>, 1 mM ZnSO<sub>4</sub>, 0.24 mM MoO<sub>4</sub>Na<sub>2</sub>, and 100 mM Na<sub>2</sub>SiO<sub>3</sub>] and grown in a growth chamber at 70% relative humidity with cycles of 16 h of light (250 μmol photons m<sup>-2</sup> s<sup>-1</sup>) and 8 h of dark at 20°C. Culture medium was replaced weekly. For water transport assays, plants were used 7 to 17 d after transfer in hydroponic culture.

### Measurement of $L_p$ in a Pressurized Chamber

The root system of a freshly detopped *Arabidopsis* plant was inserted into a pressure chamber filled with hydroponic culture medium as described (Javot et al., 2003). The rate of pressure ( $P$ )-induced sap flow ( $J_v$ ) exuded from the hypocotyl section was determined by collecting the exuded sap into a graduated glass micropipette. In practice, excised roots were subjected to a pretreatment at 320 kPa for 15 min to attain equilibration, and  $J_v$  was measured successively at 240, 320, and 160 kPa for 5 min. After flow measurements, DW<sub>r</sub> was measured. An independent set of calibration experiments was necessary to determine a relationship between DW<sub>r</sub> and overall root surface area ( $S_r$ ) calculated from measurements of the length and diameter of the root system. For these experiments, an excised root system was spread onto a clear polystyrene culture box (12 × 12 cm) and scanned, and the total length was measured using image-analysis software (Optimas-Bioscan version 6.1). For diameter measurements, the same root system was observed with a microscope at 10× magnification, and images from approximately 100 roots were taken randomly. Diameters were measured using the Optimas-Bioscan software, and their frequency repartition in 20-μm classes was determined.  $S_r$  was integrated from total root length and diameter repartition. A linear relationship between DW<sub>r</sub> and  $S_r$  was determined for each accession.

The hydrostatic water conductivity of an individual root system ( $L_{p,r}$ ; m s<sup>-1</sup> MPa<sup>-1</sup>) was calculated from the following equation using the  $J_v(P)$  relationship determined at three  $P$  values (see above):

$$L_{p,r} = J_v / (S_r \times P)$$

where  $S_r$  was deduced from a DW<sub>r</sub> measurement on the same root system. Alternatively,  $L_{p,r}$  was derived, in the inhibition experiments described below, directly from  $J_v$  measurements at the reference value of  $P = 320$  kPa. We found that  $L_{p,r}$  values measured by the two methods varied on average by less than 8% and that similar accession rankings (Fig. 1) were obtained using either method.

Acid load and respiration inhibition experiments were performed essentially as described by Tournaire-Roux et al. (2003). Briefly, root systems were

equilibrated in a standard solution [5 mM KNO<sub>3</sub>, 2 mM MgSO<sub>4</sub>, 1 mM Ca(NO<sub>3</sub>)<sub>2</sub>, and 10 mM MES, pH 6] supplemented with 20 mM KCl during 20 min at 320 kPa. Treatments were then applied by substituting the root bathing solution by the same solution but with either 20 mM KCl being substituted by 20 mM propionic acid (pH 6, with KOH) or the addition of 1 mM NaN<sub>3</sub>.  $J_v(P)$  was measured at 320 kPa during the 30 min following the treatment. For mercury inhibition experiments, roots were stabilized in the standard solution, and  $J_v(P)$  was measured at 320 kPa prior to and 40 min after the addition of 50 μM HgCl<sub>2</sub>. In all cases, the maximal percentage inhibition of  $J_v(P)$ , and therefore of  $L_{p,r}$ , was deduced by fitting the kinetic curves with a negative exponential function. For salt stress experiments, plants were incubated during 4 h in a standard hydroponic culture medium supplemented or not by 100 mM NaCl and  $L_{p,r}$  was measured as described above but with  $P$  between 400 and 800 kPa (Boursiac et al., 2005).

### Pressure Probe Measurements of $L_{p,cell}$

Cell pressure probe measurements were performed essentially as described (Javot et al., 2003). Root segments were excised from plants incubated for 4 h in a standard culture medium supplemented or not with 100 mM NaCl. The segments were bathed in a measuring solution containing 10 mM KCl and 5 mM MES-KOH, pH 6.0, in the absence or presence of 100 mM NaCl, for 10 to 40 min until successful cell impalement with the pressure probe micropipette. The measurement of cell hydraulic parameters (half-time of water exchange [ $T_{1/2}$ ], cell volumetric elastic modulus [ $\epsilon$ ], and stationary turgor pressure [ $P_s$ ]) was then completed in less than 10 min. For each of the accessions, the mean diameter and length of cortical cells were measured independently on plants grown in standard conditions using an inverted microscope at a distance of 2.0 to 4.0 mm from the apex (see values in Supplemental Table S2). The  $L_{p,cell}$  was calculated according to the following equation:

$$L_{p,cell} = \ln 2 \times V / [T_{1/2} \times A(\epsilon + \Pi_i)]$$

where  $T_{1/2}$  and  $\epsilon$  are as defined above and  $V$  and  $A$  are the cell volume and surface, respectively.  $\Pi_i$  is the intracellular osmotic pressure and was estimated from the sum of  $P_s$  and the external osmotic pressure ( $\Pi_e$ ). For each accession, cells were assumed to have the same mean dimensions under normal and salt stress conditions.

### Root Histological Analyses

Freshly harvested roots were cut into pieces of 4 to 5 mm in length at a distance of 3 or 15 mm from the apex approximately. Root pieces were fixed in 4% (w/v) paraformaldehyde (in 1× phosphate-buffered saline) for 1 h under vacuum and then stored overnight in the same, fresh solution. Roots were then washed three times in 1× phosphate-buffered saline for 15 min. Samples were dehydrated through an ethanol series (v/v: 50%, 30 min; 70%, 30 and 60 min; 95%, 2× 30 min; 100%, 2× 1 h), conserved in 100% (v/v) butanol, and embedded in Technovit 7100 (Heraeus Kulzer) according to the manufacturer's instructions. Sections of 3 to 5 μm were made with a Leitz Wetzlar rotary microtome and stained with 0.5% (w/v) toluidine blue for 1 min. For endodermis visualization, fresh roots were cut into pieces of 4 to 5 mm in length at a distance of 3 mm from the apex and incubated in 0.3% (w/v; in ethanol) Sudan IV (Carlo Erba Reagents) for 1 h. Root fragments were then rinsed in distilled water and finely chopped using a razor blade. The samples were mounted on slides in 75% (v/v) glycerol and observed at 40× with an Olympus BX61 microscope.

### Total RNA Isolation

One to 2 g of frozen roots was ground under liquid nitrogen, resuspended in 10 mL of homogenization buffer (4 M guanidine thiocyanate, 100 mM NaCl, 10 mM EDTA, 7 mM β-mercaptoethanol, 0.5% IGEPAL CA-630, and 25 mM Tris-Cl, pH 7.6), incubated for 5 min at 60°C, and centrifuged at 10,000g for 10 min at 4°C. The supernatant was extracted twice with phenol:chloroform:isoamyl alcohol (25:24:1, v/v/v), once with chloroform:isoamyl alcohol (100:1, v/v), and then precipitated with an equal volume of isopropanol in the presence of 0.3 M sodium acetate. The subsequent pellet was resuspended in 3 mL of diethylpyrocarbonate-treated water, cleared for insoluble materials, and precipitated again overnight at 4°C in the presence of 2 M LiCl and 0.5 mM MgCl<sub>2</sub>. Total RNA was recovered by centrifugation at 10,000g for 30 min at 4°C, washed with 70% (v/v) ethanol twice, resuspended in diethylpyrocarbonate-

treated water, quantified by optical density measurements at 260 nm, and stored at  $-80^{\circ}\text{C}$  until use.

## Real-Time RT-PCR

Transcript abundance was measured as described (Postaire et al., 2010). The sequences of primer pairs used for gene-specific amplification of the 13 *PIP* and four selected *TIP* genes are shown in Postaire et al. (2010) and in Supplemental Table S3, respectively. For each gene, cycle threshold values were determined in the 13 accessions of interest and relative quantification was made by the Delta cycle threshold method with correction for PCR efficiency and calibration with respect to expression in Col-0. The relative variation of transcript abundance ( $\sigma_{RE}$ ) in the 13 accessions was calculated as the  $SD$  of normalized expression data divided by mean normalized expression data in the accession set. To find the most stable reference genes between accessions or after salt treatment, several reference genes (*LIBQ10* [At4g05320], *TIP41-like* [At4g34270], *F-box family protein* [At5g15710], *ACT7* [At5g09810], *EF-1- $\alpha$*  [At5g60390], *PP2A3* [At1g13320], *SAND family protein* [SFP; At2g28390]) were investigated and their expression stability was analyzed with geNORM version 3.4 software (Vandesompele et al., 2002). *TIP41-like*, *PP2A3*, and *SFP*, on the one hand, and *EF-1- $\alpha$* , *PP2A3*, and *SFP*, on the other hand, were selected as the most stable genes among the 13 *Arabidopsis* accessions or between control and salt stress conditions, respectively. These genes were used for subsequent data normalization in the two types of experiments. Because of such normalization, the transcript abundance in Col-0 may vary slightly from 1.

## Statistical Analyses

Unless otherwise stated, all statistical analyses were conducted using Statistica software. Variations among accessions of mean physiological parameters were examined using one-way ANOVA. When a significant effect was detected ( $P < 0.05$ ), posthoc multiple comparisons were run using a Tukey test on the same set of data to identify which genotypes were statistically different ( $P < 0.05$ ). The effects of salt on water transport were assessed using an unpaired Student's *t* test. The effects of the genotype on the expression level of *PIP* genes under control conditions (Fig. 4; Supplemental Fig. S3) or their relative induction under salt stress (Fig. 9) were tested using a Kruskal-Wallis ANOVA.  $P < 0.05$  was regarded as statistically significant. For statistical multivariate analysis, PCA was performed using normalized and autoscaled data. Multiple correlation analyses among accession means were performed using Pearson linear correlation matrices, and correlations significant at  $P < 0.05$  were identified.

## Supplemental Data

The following materials are available in the online version of this article.

**Supplemental Figure S1.** Relationship among the 13 accessions between  $L_p$  and its relative inhibition by mercury, propionic acid, and azide.

**Supplemental Figure S2.** Absolute inhibition and residual values of  $L_p$  after exposure of roots to mercury-, propionic acid-, or azide-inhibiting treatments.

**Supplemental Figure S3.** Relative transcript abundance of *PIPs* in 13 accessions.

**Supplemental Table S1.** Correlation analysis of *PIP* transcript abundance versus  $L_p$ .

**Supplemental Table S2.** Water relation and morphological parameters of root cortical cells under control and salt stress conditions.

**Supplemental Table S3.** Sequences of *TIP*-specific primer pairs used for real-time RT-PCR amplification.

## ACKNOWLEDGMENTS

We thank Colette Tournaire-Roux for advice in real-time RT-PCR, Doan-Trung Doan for help in histological analyses, and Maarten Chrispeels for careful reading and editing of the manuscript.

Received July 21, 2010; accepted January 4, 2011; published January 6, 2011.

## LITERATURE CITED

- Ache P, Bauer H, Kollist H, Al-Rasheid KA, Lautner S, Hartung W, Hedrich R (2010) Stomatal action directly feeds back on leaf turgor: new insights into the regulation of the plant water status from non-invasive pressure probe measurements. *Plant J* **62**: 1072–1082
- Alexandersson E, Danielson JA, Råde J, Moparhi VK, Fontes M, Kjellbom P, Johanson U (2010) Transcriptional regulation of aquaporins in accessions of *Arabidopsis* in response to drought stress. *Plant J* **61**: 650–660
- Alexandersson E, Fraysse L, Sjövall-Larsen S, Gustavsson S, Fellert M, Karlsson M, Johanson U, Kjellbom P (2005) Whole gene family expression and drought stress regulation of aquaporins. *Plant Mol Biol* **59**: 469–484
- Alonso-Blanco C, Aarts MG, Bentsink L, Keurentjes JJ, Reymond M, Vreugdenhil D, Koornneef M (2009) What has natural variation taught us about plant development, physiology, and adaptation? *Plant Cell* **21**: 1877–1896
- Aroca R, Tognoni F, Irigoyen JJ, Sanchez-Diaz M, Pardossi A (2001) Different root low temperature response to two maize genotypes differing in chilling sensitivity. *Plant Physiol Biochem* **39**: 1067–1073
- Atwell S, Huang YS, Vilhjálmsson BJ, Willems G, Horton M, Li Y, Meng D, Platt A, Tarone AM, Hu TT, et al (2010) Genome-wide association study of 107 phenotypes in *Arabidopsis thaliana* inbred lines. *Nature* **465**: 627–631
- Baum SE, Dubrovsky JG, Rost T (2002) Apical organization and maturation of the cortex and vascular cylinder in *Arabidopsis thaliana* (Brassicaceae) roots. *Am J Bot* **89**: 908–920
- Baxter I, Hosmani PS, Rus A, Lahner B, Borevitz JO, Muthukumar B, Mickelbart MV, Schreiber L, Franke RB, Salt DE (2009) Root suberin forms an extracellular barrier that affects water relations and mineral nutrition in *Arabidopsis*. *PLoS Genet* **5**: e1000492
- Bouchabke O, Chang F, Simon M, Voisin R, Pelletier G, Durand-Tardif M (2008) Natural variation in *Arabidopsis thaliana* as a tool for highlighting differential drought responses. *PLoS One* **3**: e1705
- Boursiac Y, Boudet J, Postaire O, Luu DT, Tournaire-Roux C, Maurel C (2008) Stimulus-induced downregulation of root water transport involves reactive oxygen species-activated cell signalling and plasma membrane intrinsic protein internalization. *Plant J* **56**: 207–218
- Boursiac Y, Chen S, Luu D-T, Sorieul M, van den Dries N, Maurel C (2005) Early effects of salinity on water transport in *Arabidopsis* roots: Molecular and cellular features of aquaporin expression. *Plant Physiol* **139**: 790–805
- Bramley H, Turner NC, Turner DW, Tyerman SD (2009) Roles of morphology, anatomy, and aquaporins in determining contrasting hydraulic behavior of roots. *Plant Physiol* **150**: 348–364
- Chaumont E, Moshelion M, Daniels MJ (2005) Regulation of plant aquaporin activity. *Biol Cell* **97**: 749–764
- Chen WJ, Chang SH, Hudson ME, Kwan WK, Li J, Estes B, Knoll D, Shi L, Zhu T (2005) Contribution of transcriptional regulation to natural variations in *Arabidopsis*. *Genome Biol* **6**: R32
- Christmann A, Weiler EW, Steudle E, Grill E (2007) A hydraulic signal in root-to-shoot signalling of water shortage. *Plant J* **52**: 167–174
- Collins NC, Tardieu F, Tuberosa R (2008) Quantitative trait loci and crop performance under abiotic stress: where do we stand? *Plant Physiol* **147**: 469–486
- Daniels MJ, Chaumont F, Mirkov TE, Chrispeels MJ (1996) Characterization of a new vacuolar membrane aquaporin sensitive to mercury at a unique site. *Plant Cell* **8**: 587–599
- del Martínez-Ballesta MC, Silva C, López-Berenguer C, Cabañero FJ, Carvajal M (2006) Plant aquaporins: new perspectives on water and nutrient uptake in saline environment. *Plant Biol (Stuttg)* **8**: 535–546
- Granier C, Aguirrezabal L, Chenu K, Cookson SJ, Dauzat M, Hamard P, Thioux JJ, Rolland G, Bouchier-Combaud S, Lebaudy A, et al (2006) PHENOPSIS, an automated platform for reproducible phenotyping of plant responses to soil water deficit in *Arabidopsis thaliana* permitted the identification of an accession with low sensitivity to soil water deficit. *New Phytol* **169**: 623–635
- Henzler T, Waterhouse RN, Smyth AJ, Carvajal M, Cooke DT, Schaffner AR, Steudle E, Clarkson DT (1999) Diurnal variations in hydraulic conductivity and root pressure can be correlated with the expression of putative aquaporins in the roots of *Lotus japonicus*. *Planta* **210**: 50–60
- Hirano Y, Okimoto N, Kadohira I, Suematsu M, Yasuoka K, Yasui M

- (2010) Molecular mechanisms of how mercury inhibits water permeation through aquaporin-1: understanding by molecular dynamics simulation. *Biophys J* **98**: 1512–1519
- Höfer R, Briesen I, Beck M, Pinot F, Schreiber L, Franke R (2008) The *Arabidopsis* cytochrome P450 *CYP86A1* encodes a fatty acid omega-hydroxylase involved in suberin monomer biosynthesis. *J Exp Bot* **59**: 2347–2360
- Jang JY, Kim DG, Kim YO, Kim JS, Kang H (2004) An expression analysis of a gene family encoding plasma membrane aquaporins in response to abiotic stresses in *Arabidopsis thaliana*. *Plant Mol Biol* **54**: 713–725
- Javot H, Lauvergeat V, Santoni V, Martin-Laurent F, Güçlü J, Vinh J, Heyes J, Franck KI, Schäffner AR, Bouchez D, et al (2003) Role of a single aquaporin isoform in root water uptake. *Plant Cell* **15**: 509–522
- Mahdieh M, Mostajeran A, Horie T, Katsuhara M (2008) Drought stress alters water relations and expression of PIP-type aquaporin genes in *Nicotiana tabacum* plants. *Plant Cell Physiol* **49**: 801–813
- Martínez-Ballesta MC, Aparicio F, Pallás V, Martínez V, Carvajal M (2003) Influence of saline stress on root hydraulic conductance and PIP expression in *Arabidopsis*. *J Plant Physiol* **160**: 689–697
- Martre P, Morillon R, Barrièr E, North GB, Nobel PS, Chrispeels MJ (2002) Plasma membrane aquaporins play a significant role during recovery from water deficit. *Plant Physiol* **130**: 2101–2110
- Matsuo N, Ozawa K, Mochizuki T (2009) Genotypic differences in root hydraulic conductance of rice (*Oryza sativa* L.) in response to water regimes. *Plant Soil* **316**: 25–34
- Maurel C, Simonneau T, Sutka M (2010) The significance of roots as hydraulic rheostats. *J Exp Bot* **61**: 3191–3198
- Maurel C, Verdoucq L, Luu DT, Santoni V (2008) Plant aquaporins: membrane channels with multiple integrated functions. *Annu Rev Plant Biol* **59**: 595–624
- McKay JK, Richards JH, Mitchell-Olds T (2003) Genetics of drought adaptation in *Arabidopsis thaliana*. I. Pleiotropy contributes to genetic correlations among ecological traits. *Mol Ecol* **12**: 1137–1151
- McKhann HI, Camilleri C, Bérard A, Bataillon T, David JL, Reboud X, Le Corre V, Caloustian C, Gut IG, Brunel D (2004) Nested core collections maximizing genetic diversity in *Arabidopsis thaliana*. *Plant J* **38**: 193–202
- Melchior W, Steudle E (1993) Water transport in onion (*Allium cepa* L.) roots: changes of axial and radial hydraulic conductivities during root development. *Plant Physiol* **101**: 1305–1315
- Miyamoto N, Steudle E, Hirasawa T, Lafitte R (2001) Hydraulic conductivity of rice roots. *J Exp Bot* **52**: 1835–1846
- Munns R, Passioura JB (1984) Hydraulic resistance of plants. III. Effects of NaCl in barley and lupin. *Aust J Plant Physiol* **11**: 351–359
- Murashige T, Skoog F (1962) A revised medium for rapid growth and bioassays with tobacco tissue cultures. *Physiol Plant* **15**: 473–497
- Nienhuis J, Sills GR, Martin B, King G (1994) Variance for water-use efficiency among ecotypes and recombinant inbred lines of *Arabidopsis thaliana* (Brassicaceae). *Am J Bot* **81**: 943–947
- Paquette AJ, Benfey PN (2005) Maturation of the ground tissue of the root is regulated by gibberellin and SCARECROW and requires SHORT-ROOT. *Plant Physiol* **138**: 636–640
- Parent B, Hachez C, Redondo E, Simonneau T, Chaumont F, Tardieu F (2009) Drought and abscisic acid effects on aquaporin content translate into changes in hydraulic conductivity and leaf growth rate: a trans-scale approach. *Plant Physiol* **149**: 2000–2012
- Poormohammad Kiani S, Grieu P, Maury P, Hewezi T, Gentzbittel L, Sarrafi A (2007) Genetic variability for physiological traits under drought conditions and differential expression of water stress-associated genes in sunflower (*Helianthus annuus* L.). *Theor Appl Genet* **114**: 193–207
- Postaire O, Tournaire-Roux C, Grondin A, Boursiac Y, Morillon R, Schäffner AR, Maurel C (2010) A PIP1 aquaporin contributes to hydrostatic pressure-induced water transport in both the root and rosette of *Arabidopsis*. *Plant Physiol* **152**: 1418–1430
- Postaire O, Verdoucq L, Maurel C (2007) Aquaporins in plants: from molecular structure to integrated functions. *Adv Bot Res* **46**: 75–136
- Ren Z, Zheng Z, Chinnusamy V, Zhu J, Cui X, Iida K, Zhu JK (2010) RAS1, a quantitative trait locus for salt tolerance and ABA sensitivity in *Arabidopsis*. *Proc Natl Acad Sci USA* **107**: 5669–5674
- Rieger M, Litvin P (1999) Root system hydraulic conductivity in species with contrasting root anatomy. *J Exp Bot* **50**: 201–209
- Siefritz F, Tyree MT, Lovisolo C, Schubert A, Kaldenhoff R (2002) PIP1 plasma membrane aquaporins in tobacco: from cellular effects to function in plants. *Plant Cell* **14**: 869–876
- Steudle E (2000) Water uptake by roots: effects of water deficit. *J Exp Bot* **51**: 1531–1542
- Steudle E, Peterson CA (1998) How does water get through roots? *J Exp Bot* **49**: 775–788
- Törnroth-Horsefield S, Wang Y, Hedfalk K, Johanson U, Karlsson M, Tajkhorshid E, Neutze R, Kjellbom P (2006) Structural mechanism of plant aquaporin gating. *Nature* **439**: 688–694
- Tournaire-Roux C, Sutka M, Javot H, Gout E, Gerbeau P, Luu DT, Bligny R, Maurel C (2003) Cytosolic pH regulates root water transport during anoxic stress through gating of aquaporins. *Nature* **425**: 393–397
- Tyerman SD, Oats P, Gibbs J, Dracup M, Greenway H (1989) Turgor-volume regulation and cellular water relations of *Nicotiana tabacum* roots grown in high salinities. *Aust J Plant Physiol* **16**: 517–531
- Vandeleur R, Niemietz C, Tilbrook J, Tyerman SD (2005) Role of aquaporins in root responses to irrigation. *Plant Soil* **274**: 141–161
- Vandeleur RK, Mayo G, Shelden MC, Gilliam M, Kaiser BN, Tyerman SD (2009) The role of plasma membrane intrinsic protein aquaporins in water transport through roots: diurnal and drought stress responses reveal different strategies between isohydric and anisohydric cultivars of grapevine. *Plant Physiol* **149**: 445–460
- Vandesompele J, De Preter K, Pattyn F, Poppe B, Van Roy N, De Paep A, Speleman F (2002) Accurate normalization of real-time quantitative RT-PCR data by geometric averaging of multiple internal control genes. *Genome Biol* **3**: RESEARCH0034
- Verdoucq L, Grondin A, Maurel C (2008) Structure-function analysis of plant aquaporin AtPIP2;1 gating by divalent cations and protons. *Biochem J* **415**: 409–416
- Yu X, Peng YH, Zhang MH, Shao YJ, Su WA, Tang ZC (2006) Water relations and an expression analysis of plasma membrane intrinsic proteins in sensitive and tolerant rice during chilling and recovery. *Cell Res* **16**: 599–608
- Zimmermann HM, Hartmann K, Schreiber L, Steudle E (2000) Chemical composition of apoplastic transport barriers in relation to radial hydraulic conductivity of corn roots (*Zea mays* L.). *Planta* **210**: 302–311
- Zimmermann HM, Steudle E (1998) Apoplastic transport across young maize roots: effect of the exodermis. *Planta* **206**: 7–19